



Fourier transform absorption spectrum of $D_2^{16}O$ in 7360–8440 cm^{-1} spectral region

A.D. Bykov^b, O.V. Naumenko^b, E.R. Polovtseva^b, S.-M. Hu^a, A.-W. Liu^{a,*}

^a Hefei National Laboratory for Physical Sciences at Microscale, University of Science and Technology of China, Hefei 230026, China

^b Institute of Atmospheric Optics, Russian Academy of Sciences, Siberian Branch, Tomsk 634055, Russia

ARTICLE INFO

Keywords:

Vibration–rotation spectroscopy
 $D_2^{16}O$
 Deuterated water
 Spectroscopic parameters

ABSTRACT

The high-resolution Fourier-transform spectrum of the $D_2^{16}O$ molecule is recorded and analyzed in the region near 1.27 μm (7360–8440 cm^{-1}) where the bands of the $V=3$ ($V=\nu_1+\nu_2/2+\nu_3$) polyad are located. A total of 2772 transitions have been assigned based on recent variational calculation of Shirin et al. [JQSRT 2008;109:549–58]. A set of 1094 energy levels (564 of which are new) is determined for nine vibrational states including those of newly reported (102) and (220) states. Calculations using an effective Hamiltonian are performed to establish reasonable ro-vibrational labeling of the observed energy levels. The latest variational calculation are found to agree well with the experiment for line positions (within 0.026 cm^{-1} on average); however, the calculated intensities for transitions to upper energy levels which are in close resonance with other states can be distorted.

© 2010 Elsevier Ltd. All rights reserved.

1. Introduction

Ro-vibrational spectra of the water molecule, including its isotopologues, are essential in many applications including the evaluation of the solar radiation absorption, climate modeling, astrophysics, combustion processes, and for further optimization of variational calculations. The deuterated water, due to the large mass difference between the H and D atoms, is of particular interest.

In the last decade, high-resolution spectra of D_2O have been extensively studied with terahertz spectroscopy [1,2], Fourier-transform infrared [3–7] and intra-cavity laser absorption spectroscopy in the near-IR region [8–11]. A spectrum in the 7500–8500 cm^{-1} region, corresponding to the first decade bands ($V=\nu_1+\nu_2/2+\nu_3=3$) of the D_2O molecule, was reported in Ref. [12]. A number of $V=3$ polyad energy levels have also been reported through hot emission Fourier-transform spectroscopy ($T \sim 1500K$)

in the 2077–4323 cm^{-1} region [13]. The present study is based on new experimental measurements in the 7360–8440 cm^{-1} spectral region performed with improved signal-to-noise ratio, that allowed for the observation of a larger number of weak absorption lines. The spectral assignments are based on accurate variational calculations [14], and are also confirmed by the spectral modeling with a Watson-type effective Hamiltonian (EH). As a result, the analysis yields a considerable number of new ro-vibrational energy levels for the first decade of resonating states of $D_2^{16}O$.

2. Experimental details

The spectrum was recorded at room temperature with the a Bruker IFS 120HR Fourier-transform spectrometer equipped with a multi-pass gas cell with an adjustable path length. The whole interference chamber was evacuated to less than 0.4 mbar in order to reduce background absorption and interference from the atmospheric absorption. A tungsten source, a CaF_2 beamsplitter, and a Ge-diode detector were used in our measurements. The

* Corresponding author. Fax: +86 551 3602969.
 E-mail address: awliu@ustc.edu.cn (A.-W. Liu).

sample of $D_2^{16}O$ was purchased from PeKing Chemical Industry, Ltd. (China). The stated abundance of deuterium was 99.8%. The gas pressure was 2050 Pa, and the optical path lengths were 15 and 87 m. The sample cell had not been deuterated before recording the spectrum, thus some lines of $HD^{16}O$ and $H_2^{16}O$ can be easily found in the spectrum. Spectra recorded with larger HDO sample concentrations were also used for comparison to identify the D_2O transitions.

The unapodized resolution was 0.02 cm^{-1} , and the Boxcar apodization function was used. The line positions were calibrated using reference lines of $H_2^{16}O$ in the considered region taken from the HITRAN2004 [15] data base. The accuracy of the positions of the unblended lines was estimated to be 0.001 cm^{-1} . For illustration, small parts of the recorded spectra are presented in Fig. 1.

3. Results and discussion

The experimental linelist contained absorption features of several water isotopologues: $D_2^{16}O$, $HD^{16}O$, and $H_2^{16}O$. For the purpose of assignment, an approximate relative intensity value was derived from the peak absorption for each observed line and scaled against the calculated values [14]. By direct comparison of experimental absorption lines with the transitions which have been experimentally observed earlier or evaluated with the observed energy levels known from the literatures, the absorption lines belonging to $H_2^{16}O$ and $HD^{16}O$ were identified first, then a set of about 3000 lines presumed to belong to the $D_2^{16}O$ species was composed.

At first the $D_2^{16}O$ transitions were assigned by the comparison with the variationally calculated and

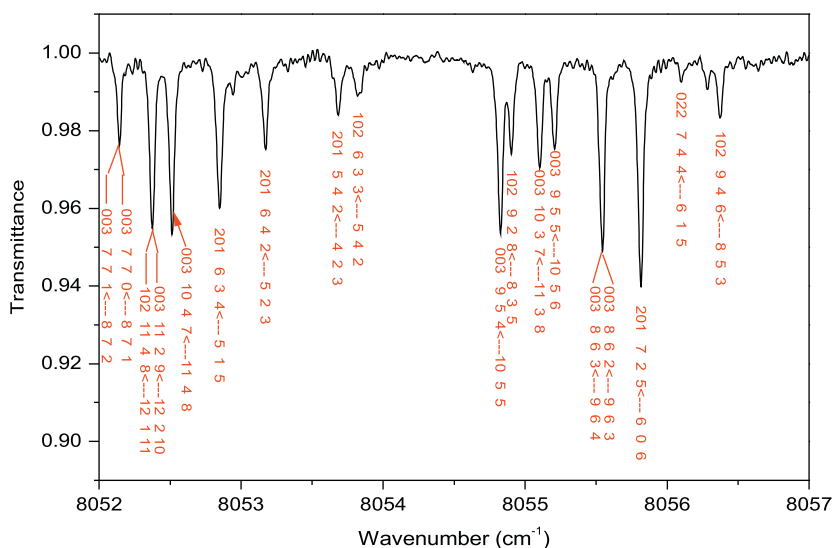


Fig. 1. $D_2^{16}O$ transitions in the region of $8052\text{--}8057\text{ cm}^{-1}$. Assignments of $D_2^{16}O$ are given. The spectrum was recorded at a pressure of 2050 Pa and equivalent absorption path length of 87 m.

Table 1

Summary of the experimental information obtained.

$\nu_1\nu_2\nu_3$	E^p , calculated, cm^{-1}	E^p , observed, cm^{-1}	Number of levels		
	Ref. [14]	This study	This paper	Ref. [12]	Ref. [13]
140	7224.69		1		
041	7343.93	$7343.92^a \pm 0.05$	48		183(37)
220	7593.25	7593.2672	104		
121	7672.92	7672.9234	168	61	77(50)
070	7771.95				
022	7826.28	$7826.29^a \pm 0.05$	42	1	127(22)
300	7852.95	7852.9292	174	57	1(1)
201	7899.83	7899.8251	219	127	27(24)
102	8054.09	8054.0742	153		1(1)
003	8220.20	8220.1793	185	111	65(38)
			1094	357	480(173)

^a Vibrational term values for the (041) and (022) states have been estimated from the *obs.–calc.* [14] trend of the $K_a=0, 1$ energy levels. The number of energy levels given in Ref. [13] common to this study is given in parenthesis.

Table 2Rovibrational energy levels of the (003), (201), (121), (300), (102), (220), (041), (022), and (140) vibrational states of D₂¹⁶O.

J	K _a	K _c	(201)				(003)				(121)				(300)			
			E	Δ	N	δ	E	Δ	N	δ	E	Δ	N	δ	E	Δ	N	δ
	1	2	3	4	5	6	7	8	9	10	11	12	13	14	15	16	17	
0	0	0	7899.8251		1	-6	8220.1792		1	-17	7672.9234		1	4	7852.9293		1	-18
1	0	1	7911.5727	0.2	2	-6	8232.0576	0.1	2	-17	7684.8451	0.4	2	4	7864.6048	0.1	2	-19
1	1	1	7918.8993	0.2	2	-7	8238.8061	0.3	2	-17	7694.5939	0.5	2	4	7872.2298	1.7	2	-20
1	1	0	7921.3210	0.2	2	-6	8241.2893	0.3	2	-17	7697.2760	0.4	2	4	7874.6172	0.1	2	-20
2	0	2	7934.5469	0.1	2	-6	8255.2380	0.2	2	-17	7708.1963	0.1	2	3	7887.4756	0.1	2	-19
2	1	2	7940.0601	0.2	3	-6	8260.0843	0.1	2	-17	7715.7761	0.1	2	3	7893.1824	0.3	4	-20
2	1	1	7947.2822	0.1	3	-6	8267.5270	0.1	2	-17	7723.8101	0.1	3	3	7900.3355	0.7	2	-19
2	2	1	7969.1555	1.1	2	-8	8287.7082	0.1	2	-18	7752.8633	0.1	2	3	7923.1070	0.1	2	-21
2	2	0	7969.6636	0.2	2	-7	8288.2763	0.1	2	-19	7753.3436	0.0	2	3	7923.5464	0.3	2	-20
3	0	3	7967.8439	0.1	2	-6	8288.7502	0.2	2	-17	7742.0958	0.0	2	2	7920.6957	0.3	3	-20
3	1	3	7971.5793	0.1	2	-8	8291.6666	0.1	2	-18	7747.2639	0.1	2	2	7924.3414	0.2	4	-20
3	1	2	7985.7973	0.1	3	-6	8306.4484	0.1	2	-16	7763.2396	0.8	3	1	7938.5592	0.0	2	-20
3	2	2	8006.1052	0.0	2	-12	8323.3646	0.1	3	-18	7788.8120	0.3	2	3	7958.0392	0.2	3	-21
3	2	1	8007.8726	0.1	3	-9	8326.0244	0.1	3	-18	7791.0865	0.3	4	2	7960.0833	0.2	2	-21
3	3	1	8047.0327	0.1	2	-8	8363.2776	0.1	2	-20	7843.4330	0.1	2	2	8001.1912	0.1	3	-21
3	3	0	8047.1017		1	-8	8363.3621	0.2	2	-20	7843.4887	0.3	2	2	8000.6134	0.3	3	-19
4	0	4	8010.6139	0.1	4	-7	8331.7510	0.0	2	-17	7785.6152	0.3	2	0	7963.4357	0.1	2	-20
4	1	4	8014.1096	0.1	2	-11	8333.2624	0.1	3	-18	7788.8050	0.1	2	1	7965.4505	0.1	2	-20
4	1	3	8036.2980	0.3	2	-6	8357.4286	0.1	2	-15	7815.0545	0.0	2	1	7988.7908	0.1	4	-20
4	2	3	8054.3163	0.1	2	-14	8370.4200	0.0	2	-18	7836.3271	0.1	3	2	8004.2656	0.1	3	-22
4	2	2	8058.7505	0.1	3	-8	8377.5017	0.0	2	-16	7842.5337	0.2	2	1	8008.9441	0.2	2	-17
4	3	2	8093.8129	0.1	2	-9	8411.7971	0.1	2	-19	7889.6651	0.1	2	8	8048.4152	0.1	2	-22
4	3	1	8094.2590	0.2	4	-10	8412.3633	0.1	2	-19	7889.9092	0.6	2	8	8046.7690	0.1	4	-18
4	4	1	8152.8993	0.5	2	-9	8465.9018		1	-23	7966.2995	0.9	2	0	8109.8142		1	-5
4	4	0	8152.9053		1	-10	8465.9131		1	-22	7966.3290		1	-1	8109.8023	0.6	2	-5
5	0	5	8062.4732	0.2	3	-8	8383.9085	0.1	3	-18	7838.2133	0.6	2	-1	8015.2697	1.1	4	-21
5	1	5	8062.7971	0.1	3	-9	8384.6192	0.1	2	-18	7840.2700	0.5	2	0	8016.2694	0.8	4	-20
5	1	4	8097.9407	0.1	3	-7	8419.5349	0.2	3	-15	7878.4799	0.1	2	-1	8050.2625	0.3	3	-21
5	2	4	8103.9151	0.3	4	4	8428.4809	0.1	2	-18	7895.1228	0.3	3	0	8061.4726	0.4	6	-22
5	2	3	8122.7255	0.2	3	-8	8442.5796	0.0	2	-15	7907.7993	0.1	3	0	8074.7894	0.8	5	-21
5	3	3	8152.5171	0.2	3	-11	8472.4394	0.3	3	-19	7948.8292	0.0	2	6	8107.9808	0.3	3	-24
5	3	2	8154.1235	0.2	3	-10	8474.5368	0.1	3	-18	7949.6435	0.1	3	8	8114.4021	0.4	3	-17
5	4	2	8211.7927	0.3	3	-12	8526.7560	0.4	2	-22	8026.2957	0.2	3	-1	8170.4446	0.5	4	-8
5	4	1	8211.8441	0.1	4	-11	8526.8462	0.3	2	-22	8026.4006	0.1	2	-1	8170.3539	0.7	3	-9
5	5	1	8286.4229		1	-17	8595.2982		1	-26	8120.5815		1	-1	8245.7208	0.3	3	-21
5	5	0	8286.4226		1	-13	8595.2979		1	-27	8120.5812		1	-2	8245.7143	0.1	2	-20
6	0	6	8123.4072	0.4	3	-9	8445.2345	0.1	2	-19	7899.7694	0.7	2	-2	8076.1448	0.0	2	-22
6	1	6	8123.5879	0.2	3	-9	8445.5817	0.1	2	-19	7899.7466	0.2	3	-2	8076.6042	0.1	2	-22
6	1	5	8169.6910	0.1	3	-8	8491.6829	0.3	2	-15	7952.4922	0.6	3	-4	8121.9986	0.3	3	-21
6	2	5	8173.4882	0.2	5	-11	8497.1296	0.0	3	-17	7965.0277	0.1	4	0	8129.2921	0.4	3	-23
6	2	4	8199.5022	0.3	4	-8	8520.6041	0.1	3	-14	7986.4916	0.1	2	-3	8151.0041	0.2	2	-22
6	3	4	8223.0898	0.1	4	-12	8544.9772	0.5	3	-18	8020.4017	0.1	3	3	8179.5926	0.3	2	-23
6	3	3	8227.1989	0.2	5	-12	8550.5176	0.0	2	-16	8033.6179	0.7	2	8	8187.3496	0.3	3	-21
6	4	3	8282.7500	0.2	4	-13	8599.9623		1	-21	8098.5371	0.2	2	-6	8243.4729	0.3	3	-8
6	4	2	8283.1619	0.2	2	-13	8600.3879	0.5	2	-21	8098.8970	0.1	3	-4	8243.1084	0.2	4	-9

Table 2 (continued)

J	K _a	K _c	(201)				(003)				(121)				(300)			
			E	Δ	N	δ	E	Δ	N	δ	E	Δ	N	δ	E	Δ	N	δ
	1	2	3	4	5	6	7	8	9	10	11	12	13	14	15	16	17	
6	5	2	8357.2497	0.1	3	-16	8668.4700	0.2	2	-22	8192.7885	0.2	2	-4	8317.8831	1	-22	
6	5	1	8357.1539	0.1	2	-16	8668.4701	1	-35	8192.7902	1.2	2	-2	8317.8365	1	-21		
6	6	1	8447.0163		1	-20	8750.9377	0.4	2	-31	8304.8642	0.3	2	-4	8408.8273	0.1	2	
6	6	0	8447.0165	0.3	2	-19	8750.9376	0.2	2	-32	8304.8641	0.1	2	-4	8408.8276	0.5	3	
7	0	7	8193.4973	0.2	2	-10	8515.8116	0.1	2	-19	7970.3404	0.1	2	-4	8146.1280	0.4	3	
7	1	7	8193.5681	0.2	3	-11	8515.8374	0.3	2	-20	7970.5613	0.4	2	-5	8146.3294	0.3	3	
7	1	6	8250.6680	0.4	3	-9	8573.0453	0.0	2	-16	8036.1288	0.1	2	-4	8203.0912	0.6	3	
7	2	6	8252.6827	0.3	5	-11	8575.9722	0.8	2	-18	8046.8181	0.0	2	0	8207.3522	0.3	4	
7	2	5	8288.3364	0.2	4	-8	8610.6535	0.2	3	-13	8077.8795	0.2	2	-5	8239.6923	0.5	2	
7	3	5	8305.3983	0.2	3	-13	8629.0520	0.3	2	-17	8104.2438	0.1	2	-2	8260.3849	0.7	3	
7	3	4	8313.5341	0.3	3	-14	8640.5897	0.5	4	-13	8122.2574	0.2	2	1	8274.4771	0.5	4	
7	4	4	8365.7994	0.4	3	-15	8685.4877	0.1	3	-21	8183.1344	0.6	2	-11	8329.2010	0.3	4	
7	4	3	8366.9568	0.5	4	-14	8686.9199	0.3	2	-19	8184.1560	0.1	3	-9	8328.1383	0.2	3	
7	5	3	8439.4402	0.0	2	-18	8753.9872	0.3	2	-24	8277.2455	1.0	2	-10	8402.1278	0.4	3	
7	5	2	8439.9921	0.5	3	-17	8754.0571	0.3	3	-24	8277.2483	0.0	2	-7	8401.8219	0.7	2	
7	6	2	8529.4465	0.5	2	-22	8836.6057	0.4	2	-29	8388.9958	0.5	2	-8	8492.8313	1.8	2	
7	6	1	8529.4470	0.6	3	-20	8836.6058	0.2	2	-30	8388.9959	0.3	2	-7	8492.8460	1	-25	
7	7	1	8634.0324		1	-31	8932.1957	0.3	2	-37	8516.9659	0.1	2	-9	8599.3796	0.1	2	
7	7	0	8634.0329		1	-30	8932.1962	0.3	2	-37	8516.9664	0.1	2	-9	8599.3795	0.1	2	
8	0	8	8272.7902	1.2	2	-10	8595.7071	0.1	2	-21	8050.0023	0.2	2	-7	8225.2807	0.2	3	
8	1	8	8272.8175	0.4	3	-12	8595.6847	0.3	2	-21	8050.1143	0.1	3	-8	8225.3628	0.4	2	
8	1	7	8340.4660	0.6	3	-11	8663.3296	0.4	2	-18	8128.6611		1	-9	8293.0581	0.4	3	
8	2	7	8341.4088	0.4	3	-12	8664.6920	0.1	2	-18	8130.6870	0.6	4	-11	8295.3175	0.3	4	
8	2	6	8388.1773	0.3	4	-9	8711.6182	0.6	2	-13	8180.9555		1	-8	8339.8500	0.1	2	
8	3	6	8399.2112	0.2	3	-13	8724.2258	0.4	2	-17	8199.8266	0.1	2	-5	8355.0037	0.1	2	
8	3	5	8428.1350	0.1	3	-9	8744.3908	1.2	2	-12	8224.9378	0.1	2	-6	8373.3135	0.3	3	
8	4	5	8460.8771	0.0	2	-15	8783.1828	0.1	2	-18	8278.0123		1	-21	8412.2806	0.4	4	
8	4	4	8463.8933	0.2	3	-15	8786.9790	0.8	2	-17	8282.5716	0.3	2	-16	8425.1926	1.0	5	
8	5	4	8534.3959	0.1	3	-18	8851.8880	0.2	2	-23	8374.0531*	0.4	2	-10	8498.5026	0.5	2	
8	5	3	8535.0848	0.2	3	-18	8852.1675	0.2	2	-22	8374.0622	0.3	2	-11	8499.4116	0.2	3	
8	6	3	8623.9276	1.0	3	-25	8934.5763	0.5	2	-25	8485.3548	0.7	3	-12	8588.7865	1.6	2	
8	6	2	8623.9248	1.7	2	-17	8934.5742	1.7	2	-37	8485.3528	1.4	2	-8	8588.8575	0.0	2	
8	7	2	8728.0379	0.8	2	-32	9030.7699	1.8	2	-33	8612.4425	0.4	2	-10	8696.4309	1	-31	
8	7	1	8728.0378	0.5	2	-29	9030.7697	2.1	2	-34	8612.4424	0.2	2	-10	8696.5416	0.7	3	
8	8	1	8846.7588	1.6	2	-44	9138.3847	1.2	2	-41	8763.6238	0.1	2	-9	8815.5209	1	-38	
8	8	0	8846.7587	1.3	2	-44	9138.3846	1.5	2	-41	8763.6237	0.2	2	-9	8815.5206	0.3	2	
9	0	9	8361.3159	1.6	2	-15	8685.0228		1	-22	8138.8002	0.1	2	-11	8313.6488	1	-26	
9	1	9	8361.3272	0.1	2	-14	8684.9118	0.0	2	-23	8138.8414		1	-11	8313.6633	1	-26	
9	1	8	8439.0946	0.1	4	-13	8762.6319	0.2	2	-18	8229.8778	0.2	2	-12	8391.4264	0.2	2	
9	2	8	8439.4888	0.2	4	-13	8763.0635	0.1	2	-19	8231.2874	0.6	2	-14	8392.9357	0.3	4	
9	2	7	8497.7366	0.2	3	-10	8822.4094	0.2	3	-13	8296.7967	0.0	2	-2	8447.8966	1	9	
9	3	7	8503.9533	0.3	3	-14	8830.0412	0.4	2	-17	8308.3636		1	-17	8459.8811	0.2	2	
9	3	6	8540.6041	0.3	3	-7	8861.0149	0.2	2	-9	8341.5041	0.5	2	-10	8487.8737	0.6	2	
9	4	6	8567.7865	0.3	3	-16	8892.7657	0.3	2	-18	8392.6581		1	-44	8522.1895*	0.3	4	
9	4	5	8574.4397	0.1	2	-15	8901.0811	0.4	3	-13	8394.3346	0.5	2	-18	8536.3095	1	-17	
9	5	5	8641.2855	0.2	4	-20	8962.1534	0.8	2	-20	8483.2878	1.9	2	-15	8607.0893	0.8	2	

9	5	4	8642.6497	0.3	3	-19	8963.0360	0.4	3	-21	8483.3713	0.4	2	-14	8607.6285	0.6	3	-21
9	6	4	8730.5630	0.1	2	-25	9044.8347	0.3	2	-27	8593.9952		1	-15	8696.6990	0.2	2	-27
9	6	3	8730.5163	0.0	2	-24	9044.8816	0.4	2	-25	8593.9796	1.3	2	-13	8696.9384	0.1	2	-27
9	7	3	8834.0792		1	-40	9141.6094	0.2	2	-35	8720.3709	0.3	3	-18	8805.7637	0.5	2	-29
9	7	2	8834.0793	0.3	2	-30	9141.6125	0.3	2	-33	8720.3711	0.6	2	-13				
9	8	2	8952.0699		1	-45	9250.9832	0.7	2	-44	8875.6742	1.3	2	-12	8924.0742		1	-40
9	8	1	8952.0698		1	-45	9250.9819	2.0	3	-45	8875.6743	1.0	2	-12	8924.0744		1	-38
9	9	1	9084.0761		1	-62	9368.7667		1	-48	9029.3007*		1	-7	9058.5102		1	-48
9	9	0	9084.0759		1	-62	9368.7667		1	-48	9029.3007*		1	-7	9058.5099		1	-48
10	0	10	8459.0765	0.2	2	-16	8784.7350		1	-24	8236.7121		1	-12	8411.1640	0.6	2	-24
10	1	10	8459.0855	0.1	3	-16	8783.9415	0.1	2	-24	8236.7521		1	-15	8411.1713		1	-27
10	1	9	8546.6915	0.1	3	16	8871.2480	0.0	2	-20	8339.8454		1	-15	8499.2823	0.1	3	-29
10	2	9	8546.8509	0.1	3	-14	8870.9802	0.2	2	-20	8340.6401	0.4	2	-16	8500.0930	0.2	2	-29
10	2	8	8619.3618	0.4	2	-18	8942.3556	1.1	2	-14	8418.7765	0.4	2	-15	8567.9595	0.3	3	-12
10	3	8	8621.4905	0.1	4	-17	8946.0865	0.1	3	-17	8427.1140	0.1	2	-18	8574.9140	0.8	2	-20
10	3	7	8665.7619	0.1	2	-5	8989.1518		1	-10	8470.9539	1.1	2	-16	8614.5508	1.7	4	-14
10	4	7	8686.0718	0.1	3	-17	9013.8510	0.1	2	-16	8509.7799	1.5	2	-24	8642.6898		1	-21
10	4	6	8698.7212	0.6	4	-17	9029.3470	0.4	2	-10	8519.5583		1	-20	8660.1595	0.5	2	-19
10	5	6	8760.0568	0.2	3	-21	9084.6813	0.0	2	-19	8604.9523*		1	-16	8727.9907	0.1	2	-22
10	5	5	8763.0177	0.0	2	-20	9087.0164	0.2	2	-20	8605.3764		1	-20	8728.5293	0.7	4	-22
10	6	5	8849.4942	0.1	3	-26	9167.3555	0.1	2	-27	8714.9988	1.4	2	-15	8816.5724		1	-26
10	6	4	8849.3403		1	-28	9167.5202	1.1	3	-26	8714.9405	3.0	2	-14	8817.1622		1	-25
10	7	4	8952.2204	1.3	2	-36	9264.6388	1.0	2	-32	8840.6832	0.5	2	-19				
10	7	3	8952.2052	7.9	2	-31	9264.6402	0.2	2	-37					8928.3859		1	-26
10	8	3	9069.5579	0.3	2	-48	9376.4028	2.6	2	-49	8999.5498	1.3	2	-10	9044.6482		1	-47
10	8	2	9069.5580	0.3	2	-50	9376.4030	2.5	2	-49	8999.5501	1.5	2	-9	9044.6508		1	-37
10	9	2	9200.4117	0.0	2	-70	9499.7379		1	-65	9152.5449*		1	-6				
10	9	1	9200.4118	0.0	2	-70	9499.7381		1	-65	9152.5451*		1	-5				
10	10	1	9361.9943	0.0	1	-102	9622.5891*		1	-56	9317.3607		1	2				
10	10	0	9361.9943	0.0	1	-102	9622.5891*		1	-56	9317.3607		1	2				
11	0	11	8566.0697		1	-17	8890.1347		1	-22	8343.8124	0.1	2	-16	8517.9181		1	-26
11	1	11	8566.0749	0.6	2	-18	8888.8730	0.1	2	-23	8343.8352		1	-19	8517.9226	0.8	2	-30
11	1	10	8663.3414	0.2	3	-16	8990.2880		1	-22	8458.6991	0.1	2	-19	8616.0919	0.5	2	-31
11	2	10	8663.3921	0.4	2	-17	8988.5807		1	-21	8459.1402	1.3	2	-19	8615.5060		1	-22
11	2	9	8745.0612	0.1	2	-14	9071.6554	0.5	2	-17	8550.8665	0.5	2	-22	8695.8964	0.6	2	-21
11	3	9	8746.4720	0.1	2	-18	9072.0448	0.3	2	-17	8555.9780		1	-19	8699.7955	0.5	3	-26
11	3	8	8801.5224	0.1	2	-3	9127.1183	1.6	2	-11	8608.7089		1	-3	8752.4409	7.2	2	-14
11	4	8	8813.4886	0.0	2	-22					8642.4405		1	-27	8773.7223	1.4	2	-21
11	4	7	8836.1004	1.0	2	-17	9171.2832		1	-6	8657.9093		1	-23	8797.8508		1	-20
11	5	7	8891.5950	0.3	4	-23	9219.2787		1	-13	8738.8356	1.8	2	-21	8861.3644	0.8	4	-22
11	5	6	8896.6434	0.4	3	-20	9224.5797	0.8	2	-13	8740.3802	0.8	2	-23	8862.0879	1.2	3	-23
11	6	6	8980.8387		1	-27					8848.3999	3.6	2	-26	8948.3775	0.1	2	-25
11	6	5	8980.4766	0.1	3	-27	9302.5578	0.2	2	-22	8848.2955	1.6	2	-18	8949.5435	0.9	2	-30
11	7	5	9082.5020	2.0	2	-36								9059.9890	1.3	3	-26	
11	7	4	9082.4509	0.2	2	-37	9399.7904	2.4	2	-33								
11	8	4	9199.2065	1.2	2	-48	9513.4763	1.7	2	-49				9177.2550		1	-43	
11	8	3	9199.2081	1.1	3	-53	9513.4760	1.9	2	-50								
11	9	3	9329.4948		1	-77												
11	9	2	9329.4951		1	-78												
11	10	2	9495.6855	0.0	1	-103					9450.5668		1	-1				
11	10	1	9495.6855	0.0	1	-103					9450.5668		1	-1				
12	0	12	8682.2086	5.2	2	-16	9008.1726	0.2	2	-22	8460.0605		1	-22	8633.8594	0.8	2	-28
12	1	12	8682.2148	0.6	2	-19	9007.4046		1	-28	8460.0994		1	-22	8633.8579		1	-39
12	1	11	8789.1322	0.2	3	-19	9111.3991	0.5	2	-24	8586.5474	0.2	2	-23				

Table 2 (continued)

J	K _a	K _c	(201)				(003)				(121)				(300)			
			E	Δ	N	δ	E	Δ	N	δ	E	Δ	N	δ	E	Δ	N	δ
	1	2	3	4	5	6	7	8	9	10	11	12	13	14	15	16	17	
12	2	11	8789.3429	0.1	2	-23	9116.4172	0.4	2	-23	8586.8379		1	-23				
12	2	10	8880.8725	0.1	2	-17	9212.4046		1	-23	8691.5189	1.1	2	-27	8831.8263	0.9	2	-24
12	3	10	8880.8990	0.4	2	-16	9207.7507	0.1	2	-18	8694.5257	0.8	2	-29	8833.9034		1	-36
12	3	9	8955.5178		1	-18	9273.6492		1	-18	8767.8719*	1.8	2	-21	8900.3516		1	-24
12	4	9	8960.7747	0.5	2	-20	9288.7385		1	-14	8786.4742	0.7	2	-29	8915.1219		1	-25
12	4	8	8985.1472	0.4	2	-25	9325.8610		1	-7	8827.2793		1	-10	8948.9890		1	-18
12	5	8	9030.6777	0.3	3	-24	9365.6276		1	-16	8885.4558	1.6	3	-29	9006.6386	0.2	4	-26
12	5	7	9043.9805	0.7	2	-20	9376.1359		1	4				9008.6812	2.1	2	-23	
12	6	7	9125.3078	0.6	2	-26	9448.8117*		1	-22	8994.2567		1	-28	9092.0090		1	-22
12	6	6	9124.1384	0.5	2	-28								9094.1010		1	-30	
12	7	6	9224.9989	1.2	2	-40	9546.9224		1	-25				9202.3500		1	-25	
12	7	5	9224.8668	1.3	2	-39	9547.0041		1	-26				9194.7549		1	-38	
12	8	5	9340.9935	1.5	2	-56												
12	8	4	9341.0526	1.1	2	-36												
12	9	4								9434.6054		1	-4					
12	9	3								9434.6052		1	-4					
12	10	3								9594.9100		1	-10					
12	10	2								9594.9100		1	-10					
13	0	13	8807.6073		1	-24	9133.7981		1	-30	8585.4979	0.4	2	-26	8758.6752		1	-34
13	1	13	8807.6119		1	-19	9133.8027		1	-30	8585.5677		1	-41	8758.8699		1	-19
13	1	12	8923.8237	0.3	2	-19	9249.8437	0.5	2	-25	8723.4635		1	-27				
13	2	12	8923.9350		1	-20	9247.2694	0.4	2	-24	8724.0153	0.8	2	-30	8875.7443	1.2	2	-15
13	2	11	9025.5729	1.0	2	-14	9352.4009		1	-29	8840.5571		1	-28				
13	3	11	9025.5250	0.2	2	-18	9353.3721		1	-23	8842.4040		1	-36	8978.6025	2.3	2	-27
13	3	10	9109.2734	0.1	2	-17	9429.0709		1	-23								
13	4	10	9112.2865		1	-21	9441.7181		1	-12				9066.4376		1	-29	
13	4	9	9164.9213	2.7	2	-25	9491.4338		1	-15				9112.6292		1	-23	
13	5	9	9195.0344		1	-27	9523.3720		1	-3	9042.9636		1	-34	9144.3860		1	-34
13	5	8	9205.1667	1.7	2	-21	9541.6861		1	-1				9168.7534		1	-6	
13	6	8												9245.9936		1	-30	
13	6	7	9280.5929		1	-28	9609.7941		1	-29				9250.9143		1	-24	
13	7	7	9379.8488		1	-43	9706.0248		1	-15				9367.5448		1	-31	
13	7	6	9379.5441	0.3	2	-40												
13	8	5	9495.3694		1	-55												
14	0	14	8942.1669	1.3	2	-26	9269.3559	0.2	2	-34	8719.1415		1	-34	8893.1717		1	-35
14	1	14	8942.1684	0.4	3	-24	9269.3574	1.0	2	-31	8719.4557		1	-33	8893.1694		1	-39
14	1	13	9067.9758		1	-23	9393.3585		1	-21	8869.5369		1	-34	9020.4329		1	-41
14	2	13	9067.9804		1	-23	9393.2630	3.0	2	-25	8869.9215		1	-36	9018.9073		1	-22
14	2	12	9179.7130		1	-28	9500.8377		1	-12	8998.2330		1	-39				
14	3	12	9179.0342		1	-21	9510.7096		1	-19	8999.9754		1	-50				
14	3	11	9273.3355		1	-19	9593.8080		1	-30								
14	4	11	9274.3632	0.3	2	-22	9604.7248		1	-15								
14	4	10	9350.7227		1	-29												
14	5	10	9360.1904	0.9	2	-26	9692.0604		1	-10				9313.1433		1	-7	
14	5	9	9379.6965		1	-25												
14	6	9	9449.5590	0.7	2	-31	9777.1330		1	-40								

14	6	8													9420.1630	1	-24	
14	7	8	9546.8685		1	-34												
15	0	15	9085.7904	0.9	2	-28	9414.1061	1	-39	8863.2915	1.8	2	-34	9036.5593	1	-37		
15	1	15	9085.9624	0.2	2	-28	9414.1067	1	-38	8863.2916	2.3	2	-45	9036.5587	1	-38		
15	1	14	9221.0652	0.0	2	-33	9547.6077	1	-30									
15	2	14	9221.1305*		1	-25	9547.6158	1	-28	9023.6281		1	-33	9172.0242	1	-32		
15	2	13	9341.5776	0.6	2	-24	9665.7126	1	-24	9164.7654		1	-48					
15	3	13	9341.5796	0.8	2	-26	9663.8039	1	-21									
15	3	12	9446.2021		1	-21												
15	4	12	9446.1631		1	-24												
15	4	11	9530.4712	1.7	2	-19												
15	5	11	9537.0850		1	-24												
15	5	10	9566.5119		1	-24												
15	7	8	9725.5449		1	-46												
16	0	16	9238.6966	0.0	2	-30	9568.0477	1	-41					9189.0370	1	-42		
16	1	16	9238.6970	0.2	2	-31	9568.0479	1	-40					9189.0363	1	-53		
16	1	15	9383.2788		1	-34								9334.0454	1	-32		
16	2	15	9383.2712	1.1	2	-29	9710.9281	1	-29	9188.0830		1	-43					
16	2	14	9513.1428		1	-29												
16	3	14	9513.1593		1	-26												
16	4	13	9627.4981		1	-24												
16	5	12	9725.0858		1	-24												
17	0	17	9400.6386	0.7	2	-34	9731.1647	1	-38					9350.6208	1	-43		
17	1	17	9400.6386	1.1	2	-33	9731.1643	1	-39					9350.6212	1	-43		
17	1	16	9554.6414	0.7	2	-33												
17	2	16	9554.6477	3.3	2	-24												
17	2	15	9693.7518		1	-31												
18	0	18	9571.6599		1	-36	9903.4471	1	-47					9521.2506	1	-47		
18	1	18	9571.6601		1	-36	9903.4473	1	-46					9521.2504	1	-48		
18	1	17												9685.1006	1	-42		
18	2	17												9685.0954	1	-49		
18	3	16	9883.3263		1	-33												
19	0	19	9751.7297		1	-42								9700.9139	1	-51		
19	1	19	9751.7302		1	-41								9700.9134	1	-52		
19	1	18	9924.3611		1	-43												
19	2	18	9924.3634		1	-40												
<i>J</i>	<i>K_a</i>	<i>K_c</i>	(102)				(220)				(041)				(022)			
			<i>E</i>	<i>A</i>	<i>N</i>	<i>δ</i>	<i>E</i>	<i>A</i>	<i>N</i>	<i>δ</i>	<i>E</i>	<i>A</i>	<i>N</i>	<i>δ</i>	<i>E</i>	<i>A</i>	<i>N</i>	<i>δ</i>
	1		2	3	4	5	6	7	8	9	10	11	12	13	14	15	16	17
0	0	0	8054.0743		1	-18	7593.2673		1	18								
1	0	1	8065.8617		1	-14	7605.1124		1	22								
1	1	1	8072.9938	1.9	2	-21	7615.3920		1	13								
1	1	0	8075.4425		1	-13												
2	0	2	8088.8912	0.6	2	-19	7628.3400	0.0	2	17								
2	1	2	8094.1235		1	-21	7636.4482	0.6	2	18	7390.8743		1	-16				
2	1	1	8101.4417	0.6	2	-19	7644.3322	0.4	2	15	7399.6012		1	-19				
2	2	1	8122.7865		1	-20	7674.9819	0.2	2	18								
2	2	0	8123.3151		1	-17	7675.4231	0.3	2	21	7440.4341		1	-12				
3	0	3	8122.2600		1	-19	7662.1453	1.5	2	15	7414.2488		1	-14				

Table 2 (continued)

J	K _a	K _c	(102)				(220)				(041)				(022)			
			E	Δ	N	δ	E	Δ	N	δ	E	Δ	N	δ	E	Δ	N	δ
1	2	3	4	5	6	7	8	9	10	11	12	13	14	15	16	17		
3	1	3	8125.5088		1	–20	7667.7574	1.2	2	16								
3	1	2	8140.0520		1	–17	7683.4604		1	15	7439.8714		1	–12				
3	2	2	8158.1553	0.6	2	–20	7710.4952		1	21								
3	2	1	8160.6281		1	–22	7712.5964	0.7	2	20	7478.3319		1	–14				
3	3	1	8199.8634		1	–27	7767.6369	0.3	2	26	7549.3915		1	–14				
3	3	0	8199.9384		1	–25	7767.6536		1	25	7549.4180		1	–26				
4	0	4	8165.1280		1	–19	7705.6365	0.3	2	14								
4	1	4	8166.8702		1	–23	7709.0702	0.3	2	11	7464.1934		1	–14				
4	1	3	8190.6908		1	–21	7734.9506	0.6	2	13								
4	2	3	8204.8628	0.2	2	–23	7757.4659		1	13	7524.3293		1	–19				
4	2	2	8211.5184	1.4	2	–22	7763.2937	1.6	2	13								
4	3	2	8247.9402		1	–14	7815.6857		1	22	7599.0055		1	–31				
4	3	1	8248.4228	0.0	2	–24	7815.8503		1	21				8042.2742	0.5	3	16	
4	4	1	8304.6178	3.7	2	–28	7896.1436	1.0	2	18	7696.6023		1	–33	8113.9887	1	–8	
4	4	0	8304.6268	0.5	2	–27	7896.0147	0.3	3	20	7696.5964		1	–42	8113.9921	0.1	2	–8
5	0	5	8217.1206		1	–22	7758.2321	0.2	2	10	7512.3883		1	–17				
5	1	5	8217.9833		1	–22	7760.1453	1.0	3	12	7515.7581		1	–22				
5	1	4	8252.5237	1.8	2	–19	7798.1052		1	3								
5	2	4	8262.5568	0.5	2	–23	7815.6036	0.9	2	9	7583.7977		1	–8				
5	2	3	8275.9156		1	–17	7827.6020	1.3	2	10	7595.8751		1	–13	8060.6241	1	7	
5	3	3	8308.0355	1.2	3	–21	7875.9098	1.2	2	18	7661.0030		1	–11	8103.0097	1	18	
5	3	2	8309.8721		1	–24	7876.6867		1	14				8105.4217	0.2	2	–1	
5	4	2	8364.8685	0.5	2	–24	7958.4911	0.1	2	14				8175.3371	1	–4		
5	4	1	8364.9340		1	–29	7957.8930	0.3	2	17	7757.8605	0.9	2	–32	8175.3793	0.8	2	–3
5	5	1	8436.7169	0.2	2	–32	8052.5128	0.7	2	34	7879.2916		1	–41	8264.2668	0.9	2	–6
5	5	0	8436.7107		1	–61	8052.5133		1	34	7879.2913		1	–43	8264.2637	3.7	2	–10
6	0	6	8278.2328		1	–22	7819.7647	1.2	2	8								
6	1	6	8278.5238	0.5	2	–21	7820.7601	0.3	2	10	7577.0091		1	–16				
6	1	5	8324.5362		1	–20	7872.0248		1	4								
6	2	5	8330.8462		1	–17	7884.5579		1	13	7654.3431		1	–20				
6	2	4	8353.1476	0.8	5	–18	7906.9085	0.4	3	3								
6	3	4	8379.9778	0.4	2	–23	7948.1733		1	10	7735.2382		1	–23	8176.0855	1.5	2	17
6	3	3	8384.9061	1.3	3	–21	7950.5134	0.6	2	8				8180.8847	1.4	2	19	
6	4	3	8437.3730	0.5	2	–27	8022.3666	0.1	2	7	7831.4588		1	–29	8249.2259	1	0	
6	4	2	8437.6905	0.7	2	–26	8031.7288	0.3	3	13				8249.4499	1	0		
6	5	2	8509.1100		1	–32	8125.7116		1	22	7953.0487		1	–41	8338.3889	1	8	
6	5	1	8509.1894	0.9	2	–30	8125.7249	0.5	2	27	7953.0782	1.4	2	–40	8338.3877	1.1	2	0
6	6	1	8595.6441	0.1	2	–37	8241.3077	1.0	2	35	8094.7921		1	–52				
6	6	0	8595.6436		1	–37	8241.3003	0.3	2	36	8094.7918		1	–56				
7	0	7					7890.2696		1	8								
7	1	7	8348.6340	0.1	2	–24	7890.7638		1	8								
7	1	6	8406.0572	2.7	2	–18	7955.7140		1	2								
7	2	6	8409.3336	1.2	4	–21	7963.9416		1	7	7735.6803		1	–22				
7	2	5	8443.1564	0.0	2	–20	7997.0944	0.8	2	0								
7	3	5	8463.4455	1.0	3	–21	8032.2341	2.0	2	4				8263.3074	0.2	2	–14	
7	3	4	8473.8782		1	–21	8036.7115	1.9	2	–4	7827.4195		1	–20	8270.7448	0.1	2	20

7	4	4	8522.1277	0.4	3	-28	8107.9256	0.0	2	5					8335.6583	0.1	3	3
7	4	3	8523.4255	0.4	2	-23	8117.4538	0.3	2	8					8336.4854	0.0	2	13
7	5	3	8593.2185	1.8	3	-30	8211.1825		1	25								
7	5	2	8593.4081		1	-23	8211.2128		1	27								
7	6	2	8680.4228	0.4	3	-34	8326.3729	0.9	2	28	8180.7992	2.0	2	-48				
7	6	1	8680.4226	0.2	2	-31	8326.3115		1	23	8180.8924	0.1	2	-50				
7	7	1	8780.6876	2.1	2	-42	8460.1862		1	37	8340.6774		1	-65				
7	7	0	8780.6875	2.3	2	-42	8460.1863		1	37	8340.6778		1	-64				
8	0	8	8428.7072	0.2	4	-23	7969.8127	0.5	2	3								
8	1	8	8428.1080	1.0	2	-25	7970.0515		1	5	7727.2278		1	-25				
8	1	7	8495.0141	1.5	3	-24	8048.4368	0.7	2	2					8284.2055	0.6	3	11
8	2	7	8497.7189	3.4	2	-21	8053.4034		1	-3								
8	2	6	8543.5539	0.6	3	-20	8099.7976	1.2	2	-3					8335.1083	2.3	2	25
8	3	6	8558.0185		1	-25	8127.7532		1	-7	7920.0238		1	-37	8359.2672	1.3	2	1
8	3	5	8576.5671		1	-26	8144.9858	0.1	2	-1	7931.2217*		1	-65	8377.2395	1.0	2	0
8	4	5	8619.0046	0.1	2	-21	8205.8906		1	1	8015.9338		1	-20	8434.5330	2.0	2	3
8	4	4	8622.2537	1.3	4	-24	8216.0889	0.6	2	6								
8	5	4	8689.0430	1.1	2	-30	8308.9580		1	11								
8	5	3	8689.4257	0.5	2	-31	8308.9950		1	15								
8	6	3	8777.1922		1	-34	8423.6318		1	20	8280.2857*		1	-32	8632.2752		1	-7
8	6	2	8777.1610		1	-42	8423.4411	0.7	2	14	8279.1569		1	-48	8632.2750		1	-11
8	7	2	8878.2580		1	-43									8748.1940		1	-20
8	7	1	8878.2583		1	-42									8748.1943		1	-20
8	8	1	8991.0725		1	-49												
8	8	0	8991.0730		1	-49												
9	0	9	8517.0107	1.7	2	-24	8058.4527		1	-1								
9	1	9	8517.0892	3.5	2	-30	8058.5580		1	-1					8291.6150	0.9	2	4
9	1	8	8594.5326	1.0	2	-23									8382.5210		1	12
9	2	8	8595.7851	0.8	2	-23	8152.6522	0.5	2	-5								
9	2	7	8654.0169		1	-20									8451.1239*		1	-3
9	3	7	8663.1942	0.1	2	-21	8234.3630		1	-6					8466.6670		1	3
9	3	6	8692.2280		1	-16												
9	4	6	8727.7113	0.8	2	-21	8315.8465		1	-2					8545.6656	0.4	2	7
9	4	5	8734.8788		1	-26	8326.7614	0.4	2	0								
9	5	5	8796.6481		1	-29	8419.1705	0.8	2	4								
9	5	4	8797.4333		1	-29	8419.1242		1	11								
9	6	4	8886.0255	0.4	2	-36	8533.0823		1	9	8388.8116	1.3	2	-21				
9	6	3					8533.1042		1	17	8389.8099	0.6	2	-38				
9	7	3	8987.5612	1.6	2	-41	8667.7217		1	28					8856.0060		1	-23
9	7	2	8987.5625		1	-36									8856.0061		1	-23
9	8	2	9103.2029		1	-56												
9	8	1	9103.2029		1	-56												
9	9	1	9225.6306		1	-68												
9	9	0	9225.6307		1	-67												
10	0	10	8613.2703	0.8	5	-26	8156.2739		1	-3	7914.6725*		1	9				
10	1	10	8612.2962	0.1	3	-23	8259.8757		1	-6	7914.8070*		1	9				
10	1	9	8703.0537	0.3	2	-27												
10	2	9	8703.4945		1	-28	8261.4205		1	-27	8038.6438		1	-25				
10	2	8	8773.2472	0.6	2	-23									8573.5658		1	6
10	3	8	8777.6105	0.3	2	-24												
10	3	7	8819.6924		1	-21												
10	4	7	8847.7478		1	-28									8668.8166	0.7	2	6
10	4	6	8861.4861		1	-24	8451.0019		1	-11								
10	5	6	8916.0326		1	-38	8542.0292	3.6	2	1								

14	3	11		9016.6102	1	–56
14	4	10				
15	0	15	9491.7482	1.1	2	–17
15	1	15	9242.4026		1	–38
15	3	13	9242.4025	0.6	2	–39
15	4	12	9617.1228		1	–19
16	0	16	9395.6073	0.4	2	–40
16	1	16	9395.6069	0.6	2	–40
			(140)			
15	6	10	9221.4747	2.0	2	–66

Note: Δ denotes the experimental uncertainty of the upper level determination (in 10^{-3} cm^{-1}). N is the number of lines used for the upper energy level determination. δ represents the deviation of the observed level from its calculated [14] value (in 10^{-3} cm^{-1}). Energies of levels marked by * differ importantly from the corresponding values of Ref. [13].

experimental line positions and intensities, then the assignments and the variational ro-vibrational labeling were further confirmed with an effective Hamiltonian approach, as discussed below.

As a result of the spectral assignment, a set of 1094 experimental energy levels has been derived for nine vibrational states of the first decade by adding the lower states (000) and (010) energies [16] to the identified transitions. A summary of the results is presented in Table 1, which also includes a comparison with the previous studies [12,13], which reported 357 and 173 energy levels in common with our data, respectively. This results in 564 new energy levels obtained in this study. The experimental energy levels derived in this study are presented in Table 2 followed by the *obs.–calc.* deviations. In fact, within the discrepancy limit $\pm 0.015 \text{ cm}^{-1}$, there are only 137 energy levels in common between this work and Ref. [13]. Detailed comparison with the energy levels derived from the hot spectrum [13] has confirmed that the values presented in here are more accurate. This is obvious for the levels derived from accurate combination differences relations. The largest discrepancies between the two data sets concern, mostly, the cases when the levels of Ref. [13] are derived from blended or single lines. Eighteen energy levels disagree with those of Ref. [13] since the absolute discrepancy varies between 0.037 and 0.135 cm^{-1} . These energy levels are marked by ‘*’ in Table 2.

Vibrational energies of the (041) and (022) states were determined from the *obs.–calc.* trend in the energy levels with $K_a=0,1$. The identification list which includes 2772 D_2^{16}O transitions is provided in the Supplementary Material (I) to this paper. For each absorption line, the experimental line position and intensity values, as well as the calculated [14] intensity and the ro-vibrational labeling are given. This list also contains 45 hot band transitions from the (010) state to the (211), (131) and (310) upper states. Information on those upper states can be found in Ref. [9]. Most (81%) of the resulting experimental intensities larger than $2.0\text{E}-25 \text{ cm/molecule}$ agree within 20% with the calculated values, while for very weak experimental lines larger discrepancy is possible.

A comparison of the observed energy levels with those calculated in Refs. [14,17] is given in Fig. 2. It is clear from the figure that recent variational calculations [14] agree very well with the experimental results with maximum *obs.–calc.* deviation below 0.10 cm^{-1} , and average *obs.–calc.* *rms* deviation of 0.026 cm^{-1} . The computations provided by Schwenke and Partridge (SP) [17] have lower accuracy for the energy levels with maximum and *rms* deviations of 0.45 and 0.17 cm^{-1} , respectively. Rotational levels in the (003) vibrational state give the most significant deviation from the SP prediction which is about -0.30 cm^{-1} .

Although there is no doubt that the new variational calculation [14] has better accuracy, the ro-vibrational labeling provided by Ref. [14] is inadequate in many cases. For this reason, we re-labeled the experimental ro-vibrational energy levels. This labeling is based on the analysis of the contributions to the ro-vibrational

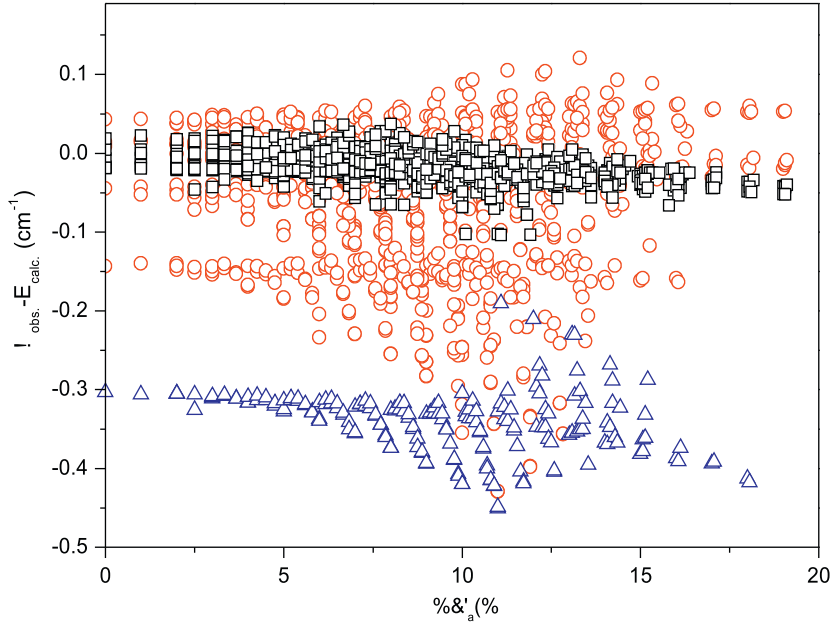


Fig. 2. Difference between the experimental and variationally computed energies of 1094 levels of $D_2^{16}O$ between 7360 and 8440 cm^{-1} , versus the quantity $J+K_a/J$. Squares: calculated values were obtained by Shirin et al. [14]. Circles: calculated values for all considered states excluding (003) state were obtained by Schwenke and Patridge [17]. Triangles: values calculated by Schwenke and Patridge [17] for the (003) state.

Table 3

'Experimental' and variationally computed rotational constants of the 1st decade of interacting states of $D_2^{16}O$.

$V_1V_2V_3$	VAR [18]	[12]	Δ_1	This paper	Δ_2
A (cm^{-1})					
041	21.169			21.182	0.013
220	17.536	17.456	-0.080	17.545	0.008
121	17.059	17.048	-0.011	17.072	0.012
022	16.619	16.857	0.238	16.631	0.012
300	14.667	14.354	-0.313	14.677	0.010
201	14.424	14.300	-0.124	14.430	0.005
102	14.261	14.551	0.290	14.255	-0.006
003	13.942	14.040	0.098	13.933	-0.009
B (cm^{-1})					
041	7.495			7.500	0.005
220	7.231	7.253	0.022	7.233	0.001
121	7.296	7.312	0.016	7.298	0.002
022	7.352	7.292	-0.060	7.359	0.007
300	7.020	6.956	-0.064	7.018	-0.002
201	7.068	7.112	0.044	7.070	0.002
102	7.099	7.186	0.087	7.113	0.014
003	7.165	7.166	0.001	7.182	0.016

Note: Δ_1 and Δ_2 are the difference between the 'experimental' values from Ref. [12] and this study and variational estimations [18], respectively.

wavefunction which have been obtained from fitting the experimental energy levels using the effective Hamiltonian method. The effective ro-vibrational operator includes the Watson-type rotational Hamiltonian in diagonal blocks:

$$H^{v\nu} = E^v + [A^v - \frac{1}{2}(B^v + C^v)]J_z^2 + \frac{1}{2}(B^v + C^v)J^2 + \frac{1}{2}(B^v - C^v)J_{xy}^2 - \Delta_K^v J_z^4 - \Delta_{JK}^v J_z^2 J^2 - \Delta_J^v J^4 - \delta_K^v [J_z^2, J_{xy}^2]_+ - 2\delta_J^v J^2 J_{xy}^2 + H_{KJ_z}^{v6}$$

$$+ H_{KJ_z}^{v4} J_z^2 + H_{JKJ_z}^{v2} J_z^4 + H_J^v J^6 + [J_{xy}^2, h_{KJ_z}^{v4} + h_{JK}^{v2} J_z^2 + h_J^v J^4] + L_{KJ_z}^{v8} + L_{KKJ_z}^{v6} J_z^2 + L_{JKJ_z}^{v4} J_z^4 + L_{KJ_z}^{v2} J_z^6 + L_J^v J^8 + [J_{xy}^2, l_{KJ_z}^{v6} + l_{JK}^{v4} J_z^2 + l_J^v J^6]_+ + \dots \quad (1)$$

The operators in the off-diagonal blocks, which describe the Fermi-type interactions, have the form of:

$$H_F^{v\nu'} = F^{v\nu'} + F_K^{v\nu'} J_z^2 + \dots + F_{xy}^{v\nu'} J_{xy}^2 + F_{xyK}^{v\nu'} [J_{xy}^2, J_z^2]_+ + F_{xyJ}^{v\nu'} J_{xy}^2 J^2 + \dots \quad (2)$$

The Coriolis-type interaction operators are

$$H_C^{v\nu'} = C_y^{v\nu'} i_y + C_{yK}^{v\nu'} [i_y, J_z^2]_+ + C_{yJ}^{v\nu'} i_y J^2 + C_{yKK}^{v\nu'} [i_y, J_z^4] + \dots + C_{xz}^{v\nu'} [J_x, J_z] + C_{xzk}^{v\nu'} [J_x^3, J_z]_+ + C_{xzy}^{v\nu'} [J_x, J_z] + J^2 + C_{xzkJ}^{v\nu'} [J_x, J_z]_+ J^2 + C_{xzyJ}^{v\nu'} [J_x, J_z] + J^4 + \dots \quad (3)$$

In Eqs. (1)–(3), $J_{xy}^2 = J_x^2 - J_y^2$ and $[A, B]_+ = AB + BA$.

The initial set of ro-vibrational parameters were taken from previous work [12]. The final fitting included all, except two, of the observed energy levels. A standard deviation of 0.0083 cm^{-1} has been achieved by adjusting 150 effective Hamiltonian parameters. In the fit, the (140) dark state has been included, as it interacts with the (041) state, while the (060) dark state is excluded since it is much lower in energy than the observed experimental energies. The rotational parameters of the (140) state have been fixed in the fitting to the corresponding values of the (041) state. All pure vibrational resonance parameters $F^{v\nu'}$ were fixed to zero because they are poorly determined due to the correlation with the vibrational term values E^v . For this reason our rotational A , B , and C constants differ from those given previously [12].

Comparison of the 'experimental' and the recent variationally computed [18] A and B rotational constants

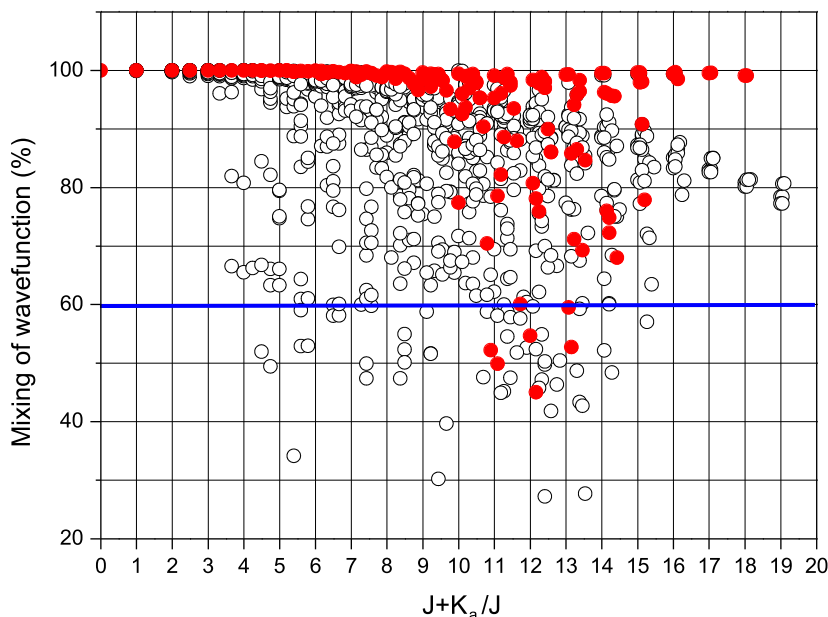


Fig. 3. Maximal mixing coefficients of wavefunctions calculated using an EH calculated versus the quantity $J+K_a/J$. Open circles: all levels excluding the (003) state. Filled circles: energy levels of the (003) state. Only 66 levels of 1094 have leading mixing coefficient not exceeding 60%.

Table 4

Experimental and calculated intensities for the $D_2^{16}O$ transitions coming on upper levels in close resonance.

	Wavenumber (cm^{-1})	Intensity (cm/mol)	Wavenumber (cm^{-1})	Intensity (cm/mol)
	(201)10 1 9 - (000) 11 1 10		(070)10 2 9 - (000)11 1 10	
Ref. [14]	7752.24	3.67E-24	7752.35	1.10E-24
SP	7752.29	4.80E-24	7751.96	7.11E-26
Observed	7752.2586	4.68E-24		
	(201)10 1 9 - (000)9 1 8		(070)10 2 9 - (000)9 1 8	
Ref. [14]	7985.92	8.69E-24	7986.03	2.59E-24
SP	7985.97	1.13E-23	7985.63	1.72E-25
Observed	7985.9375	9.69E-24		
	(201)10 1 9 - (000)10 3 8		(070)10 2 9 - (000)10 3 8	
Ref. [14]	7794.06	2.78E-25	7794.17	8.22E-26
SP	7794.08	3.61E-25	7793.75	5.64E-27
Observed	7794.0807	3.40E-25		

for the first decade of interacting states of $D_2^{16}O$ is included in Table 3. It is evident that the A and B rotational parameters obtained in this study agree very well (within 0.009 cm^{-1} on average) with the vibrationally averaged effective rotational constants evaluated in [18] based on the CVRQD potential energy surface [19].

The maximum mixing coefficient of each energy level is shown in Fig. 3. It confirms that the ro-vibrational labeling obtained within the EH approach is unique for the majority of the experimental energy levels. Only for 66 of the total 1094 energy levels, the leading mixing coefficient of wavefunction is less than 60%. Similar to the case with other isotopologues, the (003) vibrational state of $D_2^{16}O$ is less perturbed by resonance interactions with other states in the first decade, at least for $J < 10$. The

ro-vibrational labeling provided by the SP calculation coincides in most cases with the one obtained with the help of the EH calculations. Only 17 of 1094 observed energy levels are labeled differently from those provided in Ref. [17]. Our resulting labeling differs from that proposed in [14] for 142 energy levels, and only in 16 cases this can be explained by ambiguity caused by large resonance mixing of the corresponding wavefunctions.

The files with rotational, centrifugal distortion, and resonance parameters, as well as with the mixing coefficients of the resulting wavefunctions of all the vibrational states considered are given as Supplementary Material (II) to this paper.

Similar to lighter water isotopologues ($H_2^{16}O$, $H_2^{18}O$, $H_2^{17}O$, $HD^{16}O$), the $D_2^{16}O$ molecule undergoes centrifugal

distortion effect, though it is less significant than that encountered for the above isotopic species. That is why so far only a few transitions involving highly excited bending states which borrow intensity from much stronger lines—resonance counterparts have been observed in the spectra of the $D_2^{16}O$ isotopologue at room temperature. In accordance with the variational predictions [14], the (201)–(070) interaction leads to considerable strengthening of a few transitions to the rotational levels of the (070) state. Table 4 lists some of these predicted transitions. Despite the large predicted intensity (up to $2.6 \times 10^{-24} \text{ cm}^{-1}/\text{cm}^{-2}$ molecule), we could identify no transitions reaching the (070) vibrational state. At the same time, for the lines which resonance counterparts belonging to the (201)–(000) band, the calculated intensities are apparently underestimated (see Table 4). The SP intensities are also included in Table 4. It is interesting that the SP intensities match the experimental results much better for the (201)–(000) transitions, while the SP intensities for the (070) transitions are approximately an order of magnitude smaller than the results given in Ref. [14]. In fact, the summary intensity of two transitions coming on the resonating upper levels is nearly the same in both variational calculations, though its distribution between the two transitions is different in the SP and in Ref. [14]. This can be a result from different mixing coefficients of the corresponding wavefunctions in SP and in Ref. [14].

4. Conclusion

The Fourier-transform absorption spectrum of the $D_2^{16}O$ molecule has been recorded and analyzed in the 7360–8440 cm^{-1} spectral range, leading to determination of a set of 1094 energy levels for 9 vibrational states of the first decade, 564 of which are new. The (102) and (220) vibrational states are also reported for the first time. The accuracy of 173 energy levels reported previously in Ref. [13] is improved. Ro-vibrational labeling of the observed energy levels is confirmed the calculations with an effective Hamiltonian. The experimental energy levels agree better with the recent variational calculation [14] (within 0.026 cm^{-1} on average) than the SP prediction (0.17 cm^{-1} on average). However, the calculated line intensities [14] may be considerably distorted (up to an order of magnitude) for the transitions to upper energy levels in close resonance with other states.

Acknowledgments

This work was performed as part of the IUPAC Task Group (no. 2004-035-1-100) to ‘compile, determine, and validate both experimentally and theoretically, a database of water transitions’. It is jointly supported by the NSFC-China (20903085, 20873132 and 20533060), by the Chinese Ministry of Science and Technology (2007CB815203) and by RFBR (09-05-93105, 10-05-93105, 10-05-91176). The support of the Groupement de Recherche International SAMIA between CNRS (France), RFBR (Russia) and CAS (China) is also acknowledged.

Appendix A. Supplementary data

Supplementary data associated with this article can be found in the online version at doi:10.1016/j.jqsrt.2010.04.029.

References

- [1] Brunken S, Muller HSP, Endres C, Lewen F, Giesen T, Drouin B, et al. High resolution rotational spectroscopy on D_2O up to 2.7 THz in its ground and first excited vibrational bending states. *Phys Chem Chem Phys* 2007;9:2103–12.
- [2] Yu BL, Yang Y, Zeng F, Alfano RR. Terahertz absorption spectrum of D_2O vapour. *Opt Commun* 2006;258:256–63.
- [3] Toth RA. HDO and D_2O low pressure, long path spectra in the 600–3100 cm^{-1} region: II. D_2O line positions and strengths. *J Mol Spectrosc* 1999;195:98–122.
- [4] Toth RA. HDO and D_2O low pressure, long path spectra in the 600–3100 cm^{-1} region: I. HDO line positions and strengths. *J Mol Spectrosc* 1999;195:73–97.
- [5] He SG, Ulenikov ON, Onopenko GA, Bekhtereva ES, Wang XH, Hu SM, et al. High resolution Fourier transform spectrum of the D_2O molecule in the region of the second triad of interacting vibrational states. *J Mol Spectrosc* 2000;200:34–9.
- [6] Zheng JJ, Ulenikov ON, Onopenko GA, Bekhtereva ES, He SG, Wang XH, et al. High-resolution vibration–rotation spectrum of the D_2O molecule in the region near the $2\nu_1+\nu_2+\nu_3$ absorption band. *Mol Phys* 2001;99:931–7.
- [7] Ulenikov ON, Hu SM, Bekhtereva ES, Onopenko GA, He SG, Wang XH, et al. High resolution Fourier transform spectrum of D_2O in the region near 0.97 μm . *J Mol Spectrosc* 2001;210:18–27.
- [8] Hu SM, Ulenikov ON, Bekhtereva ES, Onopenko GA, He SG, Lin H, et al. High resolution Fourier-transform intra-cavity laser absorption spectroscopy of D_2O in the region of $4\nu_1+\nu_3$ band. *J Mol Spectrosc* 2002;212:89–95.
- [9] Naumenko OV, Leshchishina OM, Shirin S, Jenouvrier A, Fally S, Vandaele AC, et al. Combined analysis of the high sensitivity Fourier transform and ICLAS-VeCSEL absorption spectra of D_2O between 8800 and 9520 cm^{-1} . *J Mol Spectrosc* 2006;238:79–90.
- [10] Naumenko OV, Mazzotti F, Leshchishina OM, Tennyson J, Campargue A. Intracavity laser absorption spectroscopy of D_2O between 11 400 and 11 900 cm^{-1} . *J Mol Spectrosc* 2007;242:1–9.
- [11] Naumenko OV, Leshchishina OM, Béguier S, Campargue A. Intracavity laser absorption spectroscopy of D_2O between 12 850 and 13 380 cm^{-1} . *J Mol Spectrosc* 2008;252:52–9.
- [12] Ulenikov ON, He SG, Onopenko GA, Bekhtereva ES, Wang XH, Hu SM, et al. High resolution study of the $\nu_1+\nu_2/2+\nu_3=3$ poliad of strongly interacting vibrational bands of D_2O . *J Mol Spectrosc* 2000;204:216–25.
- [13] Zobov NF, Ovsannikov RI, Shirin SV, Polyansky OL, Tennyson J, Janka A, et al. Infrared emission spectrum of hot D_2O . *J Mol Spectrosc* 2006;240:112–9.
- [14] Shirin SV, Zobov NF, Polyansky OL. Theoretical line list of $D_2^{16}O$ up to 16 000 cm^{-1} with an accuracy close to experimental. *JQSRT* 2008;109:549–58.
- [15] Rothman LS, Jacquemart D, Barbe A, Benner DC, Birk M, Brown LR, et al. The HITRAN 2004 molecular spectroscopy database. *JQSRT* 2005;96:139–204.
- [16] Mellau G, Mikhailenko SN, Starikova EN, Tashkun SA, Over H, Tyuterev VIG. Rotational levels of the (000) and (010) states of $D_2^{16}O$ from hot emission spectra of the 320–860 cm^{-1} region. *J Mol Spectrosc* 2004;224:32–60.
- [17] Schwenke DW, Partridge H. Convergence testing of the analytic representation of an ab initio dipole moment function for water: improved fitting yields improved intensities. *J Chem Phys* 2000;113:6592–7.
- [18] Czado G, Matyus E, Csaszar AG. Bridging theory with experiment: a benchmark study of thermally averaged structural and effective spectroscopic parameters of the water molecule. *J Phys Chem* 2009;113:11665–78.
- [19] Barletta P, Shirin SV, Zobov NF, Polyansky OL, Tennyson J, Valeev EF, et al. CVRQD ab initio ground-state adiabatic potential energy surfaces for the water molecule. *J Phys Chem* 2006;125:20437–55.